Orthopedics and Rheumatology
Open Access Journal
ISSN: 2471-6804

Research Article
Volume 22 issue 1 - July 2023
DOI: 10.19080/OROAJ.2023.22.556076

Ortho & Rheum Open Access J

Physiochemical Dissolution Governs Early Modifications in Acid-Exposed Murine Bone with Long-term Recovery

Mikayla Moody[1], Anna Peterson[1], Brian Wingender[1], Katya Morozov[1], Iris Nakashima[1], Margaret Easson[1], Ron Abraham[1], Tannin Schmidt[1], Leslie Caromile[2], Ernesto Canalis[3] and Alix Deymier[1]*

[1]*Department of Biomedical Engineering, School of Dental Medicine, University of Connecticut Health Center, USA*

[2]*Department of Cell Biology, School of Medicine, University of Connecticut Health Center, USA*

[3]*Department of Orthopedic Surgery and Medicine, UConn Musculoskeletal Institute, University of Connecticut Health Center, USA*

Submission: June 22, 2023; **Published:** July 05, 2023

***Corresponding author:** Alix Deymier, Department of Biomedical Engineering, School of Dental Medicine, University of Connecticut Health Center, Farmington, CT, USA

Abstract

Metabolic acidosis (MA), a disease affecting millions annually, is clinically characterized by a decrease in systemic pH and bicarbonate. MA has been shown to have skeletal consequences, such as increased bone loss and fractures. However, the mechanisms impacting the mechanics of bone remain unknown. To determine this, we characterized the skeletal phenotypes resulting from two independent regimes of ammonium chloride (NH_4Cl) acid-dosing in skeletally mature CD-1 mice for 1, 3, 7, and 14 days to establish the temporal progression of materials-level skeletal defects. The classical, flat-dose model resulted in a temporary decrease in blood pH but did not reduce blood bicarbonate levels. Minimal alterations were observed in bone composition, structure, mechanics, and cellular behavior. However, the graded administration of NH_4Cl maintained MA for up to 14 days. This resulted in decreased bone mineral content, collagen organization, and bone volume while increasing mineral crystallinity at early time points followed by a return to baseline. Changes to the matrix lead to a potential decrease in bone toughness at early time points, which may explain the increased fracture risk seen clinically. However, there were no changes in bone formation rate nor osteoclast number or activity during any time point. After 14 days, the bones were fully recovered even though the mice were still under acidotic conditions. Ultimately, we conclude that physicochemical dissolution is the main mechanism for early changes in murine bone, which is influenced by the dosing of exogenous acid loading. This knowledge will aid the discovery of treatments that prevent acidosis-induced bone dissolution.

Keywords: Acidosis; Physiochemical Dissolution; Biomechanics; Bone Composition; Bone Structure

Introduction

Bone health is heavily dependent on its environment, including the composition of the surrounding body fluid. Pathological changes such as those seen with metabolic acidosis (MA), which is characterized by reduced blood pH and bicarbonate (HCO_3^-) content, have been shown to be detrimental to bone structure and function [1-4]. MA promotes decreased bone mineral density (BMD) and increased fractures risk that affect thousands of individuals in the US and millions of individuals globally each year [5,6] with enormous medical costs [7,8]. Concerns about the effect of acidosis on bone health are only growing due to the prevalence of acidic diets, the rising number of patients with chronic kidney disease and diabetes, and an aging population, all correlated with a lowered physiological pH [9-11]. Therefore, there is a significant need to understand the mechanisms of MA that induce compromised bone health. Two critical factors to fulfilling this need are:

i. Developing relevant animal models for research and

ii. Understanding the dose and time dependence of bone's response to acidosis.

Previous animal models of MA have sought to induce the condition via clinically relevant [12] administration of a flat-dose of ammonium chloride (NH_4Cl) model [13-21]. Although mouse studies were able to successfully induce acidosis in the short term (1-3 days), a lot of the acidosis maintenance was limited by day 7 [18,20]. In addition, one study using a flat-dose model showed

no changes in bone [20]. It has been unclear whether this lack of effect is caused by low dosage or limited experimental time. Our lab created a graded-dose murine model of NH_4Cl in the drinking water in which the administered dose increased stepwise throughout the experimental course [22]. This model-maintained acidosis at 14 days and induced changes in bone composition and mechanics pointing to its value as a model to replicate bone phenotypes seen in clinical MA. Although valuable, the temporal effects of this graded dosing on murine bone composition, structure, and function have not been examined.

Bone is a mineralized tissue that not only provides structural integrity and mobility to the body, but also acts as the body's largest ion reservoir [1,23,24]. It is composed primarily of carbonate-substituted calcium apatite, collagen, water, and cells [25,26]. Changes to the composition, structure, and organization of these components, known as bone quality, will significantly affect its mechanical function [27,28]. In the case of MA, the reduced blood pH and HCO_3- levels prompt the dissolution of bone, thus releasing buffering ions to increase the pH back to homeostatic levels. In chronic MA, two primary processes of bone dissolution have been identified: short-term physiochemical dissolution, via interactions between protons and bone material, and long-term cell-mediated resorption, caused by acid-induced osteoclast differentiation and activity [22,29-41]. However, the temporal and dose-dependence of these mechanisms *in vivo* remains unknown. MA can either last for several hours to days up to many months and years in humans [42]. Therefore, it is important to use available murine models to try and understand the temporal contributions of physiochemical and cell-mediated processes on acidosis-induced bone quality degradation.

In this study, we compare the effects of both the flat-dose and graded-dose models of NH_4Cl administration on bone quality and mechanics in CD-1 mice. We use a multi-modal approach to measure spatial changes in bone composition and structure and their consequences on the tissue mechanics as a function of time up to 14 days. This study seeks to validate current murine models of MA as well as establish dose and time dependent consequences of MA on bone quality and function. These results are important not only for those studying acidosis, but also for research into other conditions such as hypertension [43,44], pancreatitis [45], and chronic kidney disease [46] in which acidosis may appear as a comorbidity.

Materials and Methods

Induction of Metabolic Acidosis

All animal experimental procedures were approved by the Institutional Animal Care and Use Committee at UConn Health Center and Columbia University and comply with the National Institutes of Health guide for the care and use of laboratory animals (NIH Publications No. 8023, revised 1978). 4-6-month-old male CD-1 mice (Charles River Laboratories, Worcester, MA) were separated into 4 groups: flat-dose and graded and their respective controls. Within the flat-dose and graded-dose groups, the mice were further divided into separate time points representing the time of sacrifice after acidosis induction: day 1, day 7, and day 14 for flat-dose with an additional day 3 for graded-dose. Control mice were housed in adjoining cages and had no changes in diet for the extent of the experiment. Our previous studies showed that control mice exhibited no changes over the course of 14 days; therefore, they were sacrificed throughout the experiment but not necessarily on days equivalent to Days 1, 3, 7, and 14 [22]. Metabolic acidosis was induced in flat-dose and graded-dose mice by replacing their drinking water with an aqueous solution of ammonium chloride (NH_4Cl) and 5% sucrose. For the flat-dose group, the NH_4Cl dose remained constant at 0.28 M for 14 days as per Nowik et al. [13]. For the graded-dose group, the NH_4Cl dosing began at 0.2M and was increased by 0.1 M every 3 days for 14 days as per our previously established graded model [22]. Water consumption and weights were measured every 3 days for the graded-dose mice. To evaluate the temporal effects of acidosis on bone, the mice were sacrificed at their assigned time point via CO2 asphyxiation, which was followed by femur collection. The femurs were characterized by (1) mechanical, (2) structural, (3) compositional, and (4) cellular properties (Figure S1).

Blood and urine chemistries and assessment of acidosis

Confirmation of acidosis induction and evaluation of mouse health was determined by blood analysis for both groups with additional urine analysis for the graded-dose mice. For all mice, blood gas testing was performed on the day of sacrifice immediately prior to sacrifice. For blood chemistries, 200-300 μL of blood was extracted from non-anesthetized mice via submandibular puncture procedures [47]. To control any potential reduction of CO_2, blood samples were obtained and immediately processed using a Heska PoC Epoc blood-gas analyzer (Loveland, CO, USA) to obtain values of blood pH, partial pressure of O_2, partial pressure of CO_2, as well as ion concentrations of HCO_3-, calcium, sodium, and chloride along with metabolic indices including lactate and glucose. Urine pH was measured for the graded-dose group only using colorimetric pH strips with a 0.5 pH unit resolution (Hydrion, Brooklyn, NY) starting on the day of acidosis induction (day 0) and every 3 days thereafter for the duration of the experimental timeframe.

Assessment of bone tissue composition

Raman spectroscopy was used to evaluate the composition of both the femoral surface and interior using a Witec alpha 300 Raman Spectrometer (Witec, Ulm, Germany). Samples were obtained and processed as previously described (n=3 mice/time point) [22]. For the external surface measurements, the anterior surface of intact femurs was cleaned of all soft tissue, including the periosteum, by manual clearance of tissue with a scalpel blade

How to cite this article: Mikayla M, Anna P, Brian W, Katya M, Iris N, et al. Physiochemical Dissolution Governs Early Modifications in Acid-Exposed Murine Bone with Long-term Recovery. Ortho & Rheum Open Access J. 2023; 22(1): 556076. DOI: 10.19080/OROAJ.2023.22.556076

and buffing with fine grained sandpaper. Five measurements were then taken across the bone in a medial-lateral direction with a 50X objective at each of three locations along the bone: proximal, distal, and mid-shaft, using a 785 nm laser with a laser power of 65mW or less, and an acquisition time of 2 x 30 seconds. After the surface measurements, the bones were mounted in Optimal Cutting Temperature (OCT) medium and frozen at -80°C. The bones were then cryosectioned along the coronal plane into 20 µm thick frozen sections using the tape method for mineralized tissues [48]. For the internal samples, six measurements on the cortical bone interior were made at each of three locations: midshaft, proximal, and distal, where the latter two were located ~2 mm above and below the midshaft location. Acquisition parameters were consistent with the surface measurements. The spectra collected at each location were cropped to 200-1800 cm^{-1}, background corrected, and averaged into a single spectrum using Witec Project 5.1. Peak fitting was performed using 8 peaks and assuming a Lorentzian shape function in the Witec Program 5.1 integrated fitting software (Figure S2). The resultant areas of the fitted peaks were used to calculate bone composition values. The ratio of the 960 Δcm^{-1} ν1 phosphate in apatite peak and the 1003 Δcm^{-1} phenylalanine collagen peaks were used to determine the mineral: matrix ratio. The bone carbonate content is defined as the area ratio of the 1070 Δcm^{-1} carbonate in apatite peak and the 960 Δcm^{-1} ν1 phosphate (PO_4) in apatite peak, known as the carbonate: phosphate (CO_3:PO_4) ratio. In addition, we fitted peak ratios for CH_2 wag and amide I (Table S1).

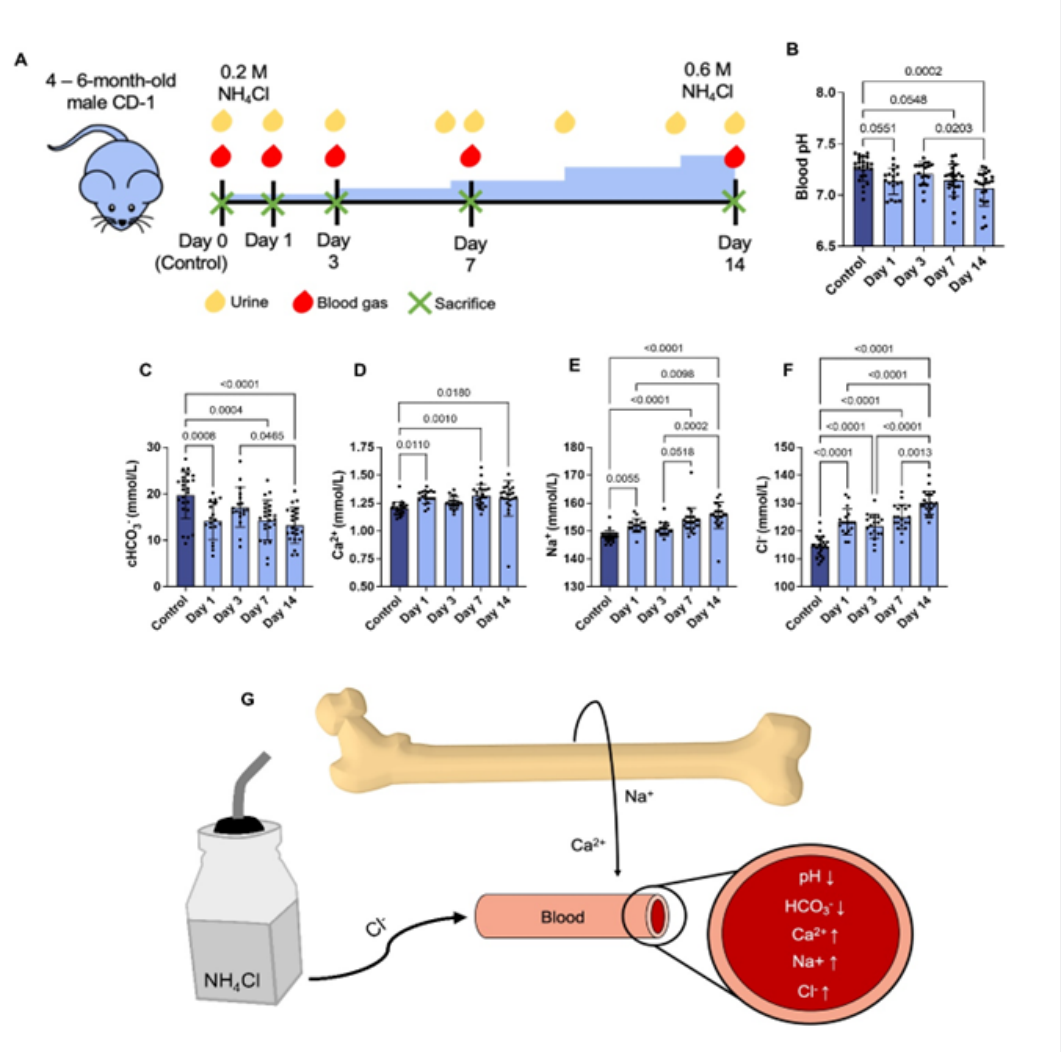

Figure 1: Graded dosing of ammonium chloride creates a time-dependent expression of chronic metabolic acidosis in mice. (A) A schematic illustrating the experimental design for graded dosing as well as urine and blood collection. For each timepoint, blood collected was analysed for (B) pH, (C) bicarbonate (HCO_3-), (D) calcium (Ca^{2+}), (E) sodium (Na+), and (F) chlorine (Cl^-). (G) A schematic showing the effects of an ammonium chloride (NH_4Cl) liquid diet has on the vascular and skeletal systems. One-way ANOVAs and post-hoc Tukey's tests were used. P values less than or equal to 0.1 are reported.

How to cite this article: Mikayla M, Anna P, Brian W, Katya M, Iris N, et al. Physiochemical Dissolution Governs Early Modifications in Acid-Exposed Murine Bone with Long-term Recovery. Ortho & Rheum Open Access J. 2023; 22(1): 556076. DOI: 10.19080/OROAJ.2023.22.556076

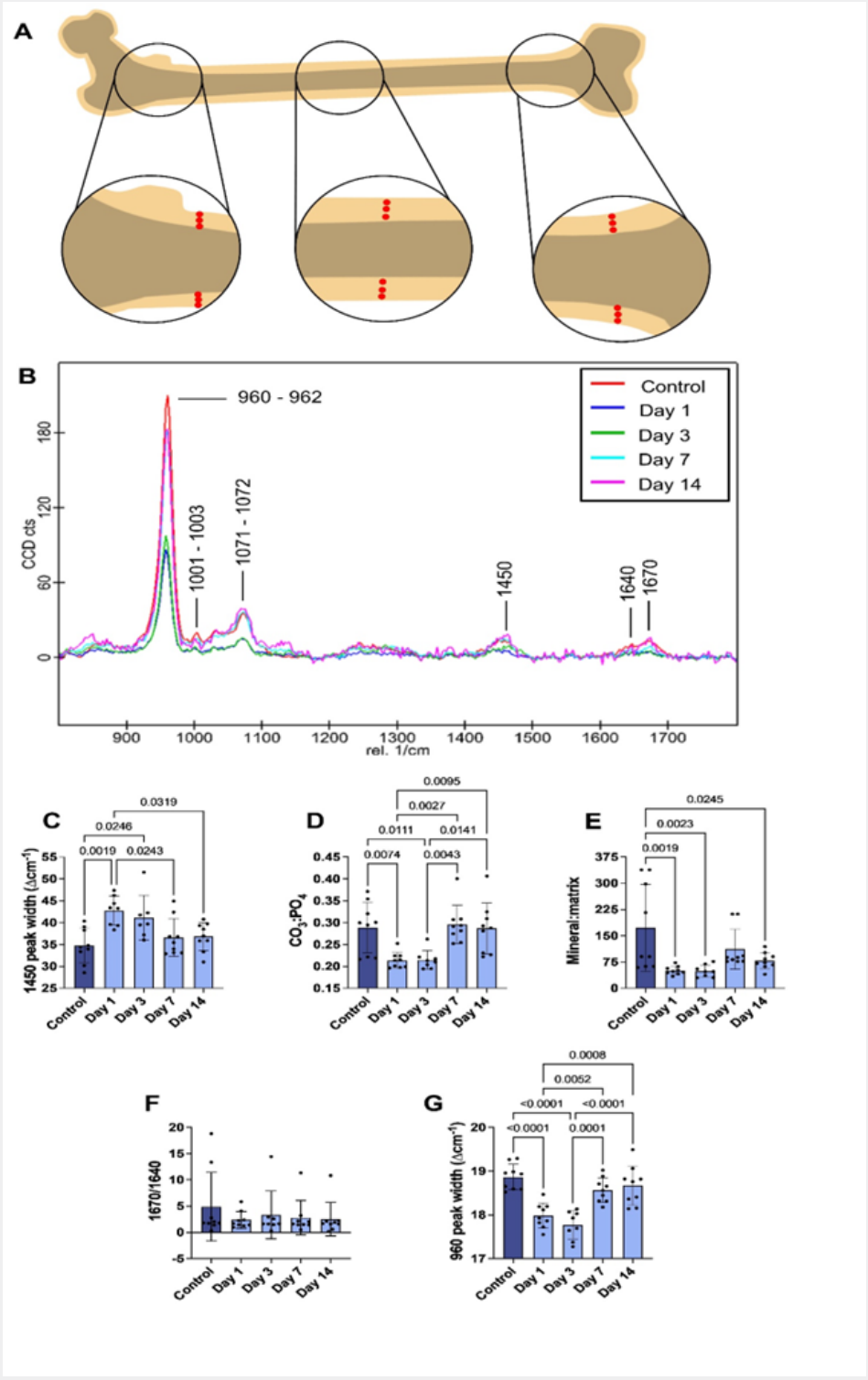

Figure 2: Interior composition of murine bone exposed to acid experienced a reduction in carbonate (CO_3) and an increase in collagen denaturation at early timepoints. (A) A schematic showing where spectra were taken on sectioned bone slices, as indicated by the red dots. (B) Raman spectra were then used to calculate (C) 1450 peak width, (D) carbonate: phosphate ratio (CO_3:PO_4), (E) mineral:matrix, (F) 1670/1604 ratio, and (G) 960 peak width. One-way ANOVAs and post-hoc Tukey's tests were used. P values less than or equal to 0.1 are reported.

How to cite this article: Mikayla M, Anna P, Brian W, Katya M, Iris N, et al. Physiochemical Dissolution Governs Early Modifications in Acid-Exposed Murine Bone with Long-term Recovery. Ortho & Rheum Open Access J. 2023; 22(1): 556076. DOI: 10.19080/OROAJ.2023.22.556076

Evaluation of whole-bone mechanics

3-point bend tests were used to evaluate the mechanical properties of the femurs. Samples were obtained and processed as previously described [22] (n=10-15 mice/time point). Femurs were placed into a Biomomentum Mach-1 3-point bend Mechanical testing rig (Biomomentum, Laval, Canada) with the posterior side facing up to induce fracture on the anterior side. The span across the beams was 8 mm and the femurs were loaded at a rate of 0.1 mm/s until failure using a 25 kg load cell. Samples were immersed in phosphate buffered saline maintained at body temperature (37°C) throughout testing to replicate *in vivo* conditions and maintain hydration. Applied force was recorded from the load cell and platen displacement was used as a measure of sample displacement. Measurements of bone cross-section, moment of inertia, and centroid distance were measured using microcomputed tomography (μCT) as described in the next section. Load vs. displacement curves were analyzed using custom programs in MATLAB to determine structural mechanical properties, such as stiffness, maximum load, and work to fracture. Stress vs. strain curves were calculated by normalizing the force and displacement using the beam span length, the bone centroid distance, and the area moment of inertia. Material mechanical properties were calculated from these plots to obtain modulus, maximum stress, resilience, and toughness.

Structural analysis using microcomputed tomography

After mechanical testing, the femoral samples were evaluated by microcomputed tomography (μCT) to obtain structural information for the region of fracture, the cortical midshaft, and the distal trabecular bone. Samples (n=7-15 mice/time point) were obtained and processed as previously described [22]. Bones were dehydrated using graded ethanol rinses and then imaged with a Scanco 40 μCT system (μCT 40, Scanco Medical, Bruttisellen, Switzerland) located in the UConn Health MicroCT Imaging Facility using a resolution of 16 μm. For the fracture region, scans were collected over a region spanning +/-2 mm around the fracture site. From these scans, the 30 μCT sections immediately adjacent to either side of the fracture site were isolated and analyzed using the BoneJ toolbox of ImageJ [49] (U. S. National Institutes of Health, Bethesda, Maryland, USA) to determine centroid distance and area moment of inertia of the bone at the fracture site. The values for femur centroid distance and area moment of inertia were used to normalize the mechanical data as described above. The trabecular parameters were measured from μCT slices at the distal epiphysis of the femur distal to the growth plate and within the distal shaft in a region 160 μm proximal from the distal growth plate. This region of interest was selected, thresholded, and analyzed using Bruker CTAn software to obtain bone volume/total volume (BV/TV), trabecular separation (Tb.Sp), trabecular thickness (Tb.Th), and trabecular number (Tb.N). For cortical thickness (Ct.Th), the region of interest was composed of 100 slices located ~1 mm above the distal growth plate and was isolated and analyzed using Bruker CTAn software. The cortical and trabecular segmentation procedures included thresholding, despeckling, ROI shrink-wrapping, and morphological operations. Some samples that underwent mechanical testing were omitted from μCT analysis either due to trabecular bone breakage within in the distal epiphysis, the presence of a crack in the region of interest for the cortical bone, or the sample was used for another analysis technique.

Bone dynamic histomorphometry

Five mice per experimental group received intraperitoneal injections of calcein (2.5mg/mL) and alizarin complexone (3mg/mL) 7 and 2 days before sacrifice, respectively (Sigma-Aldrich, St. Louis, MO). Because of this necessary time delay between injections, dynamic histomorphometry was not performed on mice from the day 1 or day 3 time point. These fluorescent dyes attach to the mineralizing bone surface thus acting as markers for bone remodeling or deposition occurring between injection dates [22,48]. At the time of sacrifice, the femurs were immediately excised and fixed in 4% paraformaldehyde (PFA) followed by sucrose fixation. Samples were then mounted in OCT, frozen at -80°C, and cryosectioned into 7 μm thick sections along the coronal plane using a Leica CM3050-S cryostat. The sections were analyzed using the OsteoMeasure (OsteoMetrics, Atlanta, GA, USA) image analysis system to determine the double label surface (dLS), single label surface (sLS), Mineral Apposition Rate (MAR) and Bone Formation Rate (BFR). Due to animal loss and sample loss during processing, the sample sizes for this technique decreased to about a n=2-3 mice/time point.

Tartrate-resistant acid phosphatase (TRAP) staining

Traditional non-fluorescent TRAP histological staining was also performed on femurs (n=4-16 mice/time point). The femurs were dissected immediately after sacrifice and fixed in 4% PFA at 4°C for 24 hours, followed by dehydration using graded ethanol rinses. The femurs underwent demineralization using EDTA prior to traditional tartrate resistant acid phosphatase (TRAP) staining and methyl green counterstaining (Sigma) as described previously [22]. TRAP+ cells in trabecular bone were analyzed using the OsteoMeasure (OsteoMetrics, Atlanta, GA, USA) image analysis system to obtain osteoclast (Oc.N) number and osteoclast (Oc.S) surface relative to measurements of bone surface (BS) [44]. Due to animal loss and sample loss during processing, the sample sizes for this technique decreased from the original n=10-16 mice/time point.

Statistical analysis

For quantitative outcomes, statistical analysis was done by using one-way ANOVAs with the use of Minitab and GraphPad Prism version 9.2.0 software. A significance level of at least 0.05 was used for all tests. Comparisons between groups over time

How to cite this article: Mikayla M, Anna P, Brian W, Katya M, Iris N, et al. Physiochemical Dissolution Governs Early Modifications in Acid-Exposed Murine Bone with Long-term Recovery. Ortho & Rheum Open Access J. 2023; 22(1): 556076. DOI: 10.19080/OROAJ.2023.22.556076

were made using one-way ANOVAs and post-hoc Tukey's tests. GraphPad Prism version 9.2.0 was used for data visualization of raw data with a selection of statistical summaries. P values less than or equal to 0.1 were reported on graphs, while significance was established as $p<0.05$. Correlations were calculated between blood gas, compositional, structural, and mechanical parameters to determine any linear relationships (Table S3).

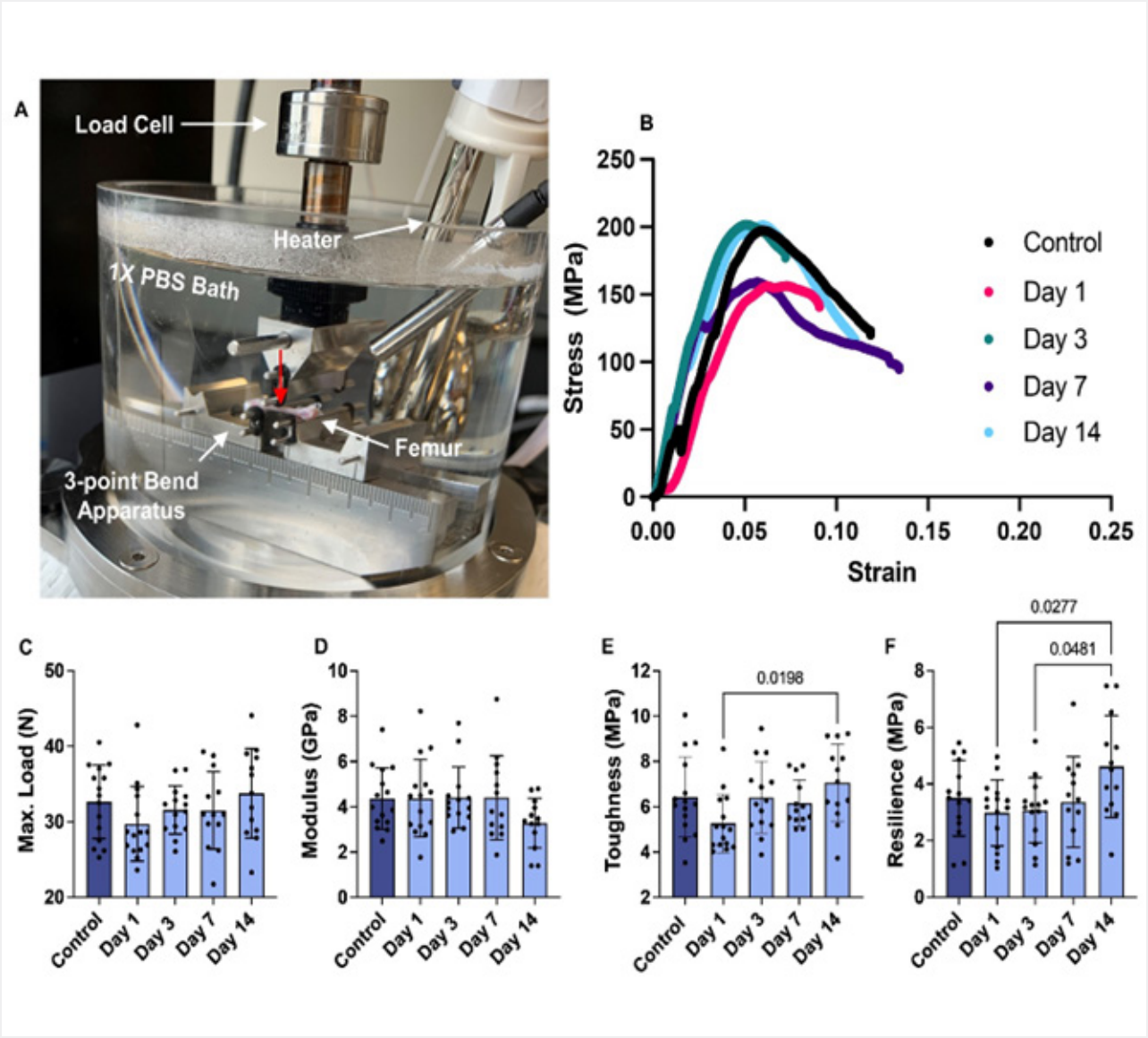

Figure 3: Mechanical properties recovered after 14 days of acidosis induction. (A) The set-up from 3-point bend testing for femoral samples. The red arrow indicates the direction of the top point during the test. (B) Stress vs. strain curves were used to calculate various mechanical parameters, including (C) maximum load, (2) modulus, (E) toughness, and (F) resilience. One-way ANOVAs and post-hoc Tukey's tests were used. P values less than or equal to 0.1 are reported.

Results

Blood gas ion analysis showed diets induced different durations of MA

The progression of the acid-base dysregulation with either flat-dosing or graded-dosing of NH_4Cl was determined by monitoring altered blood-gas values over the course of two weeks (Figure 1, S3, S4). Mice on the graded-dose diet regimen (Figure 1A) exhibited significantly reduced blood HCO_3- and pH at late time points (days 7 and 14) compared to its control, indicating that long term acidosis was successfully induced. At day 1, HCO_3- levels were also reduced to 14.17 mmol/L compared to a control level of 19.75 mmol/L; however, there was only a trending decrease in the blood pH (Figure 1B-C). This is followed by a

How to cite this article: Mikayla M, Anna P, Brian W, Katya M, Iris N, et al. Physiochemical Dissolution Governs Early Modifications in Acid-Exposed Murine Bone with Long-term Recovery. Ortho & Rheum Open Access J. 2023; 22(1): 556076. DOI: 10.19080/OROAJ.2023.22.556076

return to baseline levels for both pH and HCO_3- at day 3 (Figure 1C). There was a strong correlation between the blood pH and the HCO_3- level (C=0.88).

The flat-dose mice group exhibited a significant decrease in pH after 1 day of NH_4Cl-dosing compared to its control (Figure S3A). However, following day 1 of acidemia, the pH returned and was maintained at levels similar to the control throughout the remaining experiment. The flat-dose group showed no change in blood HCO_3- levels compared to its control (10.82 mmol/L) at any time point, but HCO_3- levels increased to 12.29 mmol/L and 11.92 mmol/L for days 7 and 14 compared to day 1 (7.431 mmol/L) (Figure S3B).

Blood ion levels were also modified in response to the dosing and duration of NH_4Cl administration. Blood calcium (Ca2) and sodium (Na^+) were monitored as elevations in these ions are associated with changes in skeletal tissue [50,51]. In the graded-dose group, Ca^{2+} and Na^+ levels significantly rose at all time points except day 3 (Figure 1D-E). The flat-dose group had significant increases in blood Ca^{2+} at days 1 (1.226 mmol/L) and 14 (1.203 mmol/L), with a return to normal levels at day 7 (1.148 mmol/L), compared to the control (1.099 mmol/L) (Figure S3C). Additionally, Na+ increased at days 1 (153 mmol/L) and 7 (151.7 mmol/L) compared to its control group (148.7 mmol/L).

To establish consumption of ammonium chloride (NH_4Cl) and its effect on the health of the animals, we also evaluated the chlorine (Cl^-) concentration in the blood in addition to murine weight and the volume of liquid consumed by the mice during standardized water changes. As anticipated with ammonium chloride supplementation, blood Cl^- levels were significantly increased for all time points compared to the controls for both flat (119.8 mmol/L to 124.2 mmol/L) and graded-dose (114.6 mmol/L to 130.1 mmol/L) groups (Figure S3E & 1F). The graded-dose mice also began to significantly lose weight starting on day 12 (38.82 g) compared to day 0 (42.78 g) and drank less liquid at higher concentrations of ammonium chloride (4.852 mL at 0.6M compared to 8.574 mL at 0.2M) (Figure S5A-B). However, weight loss was not large enough to perturb quality of life nor justify sacrifice due to poor health. The progression of the acid-base imbalance was also assessed by urine pH measurements. Urine pH of the graded-dose mice remained significantly low at all time points (pH 5.912 by day 14) compared to its control and day 0 groups (pH 6.895 and 6.793, respectively) (Figure S5C)

Assessment of internal and external bone tissue composition in response to acid-loading

Raman spectroscopy was used to assess compositional changes on the exterior surface (Figure S7A) and internal cross-sections (Figure 2A) of bone tissue. In the graded-dose group, we observed that systemic acid-loading significantly altered bone tissue composition. For the bone interior, the CO_3:PO_4 ratio and 960 cm^{-1} peak width lowered at days 1 and 3 while the 1450 cm^{-1} peak width rose at these same time points (Figure 2C, D & G). These indicate a decrease in bone carbonate content [52], an increase in bone mineral crystallinity [53, 54], and an increase in collagen structural disorder [53], respectively. In addition, the mineral: matrix ratio significantly decreased at days 1, 3, and 14 (Figure 2E). For the bone exterior, CO_3:PO_4 decreased, and the 1670/1640 ratio—a collagen denaturation marker [55]—increased at day 14 compared to control but showed no change in the mineral:matrix ratio at any time point (Figure S7). The bone interior for the flat-dose model exhibited a significant decrease in CO_3:PO_4 and a trending decrease in the mineral:matrix ratio at day 1 compared to the control, followed by a return to control levels at days 7 and 14 (Figure S6B-C). However, these results were not mirrored on the bone exterior where the only significant changes were a decrease in the width of the 1450 cm^{-1} peak at day 1 and a trending increase in CO_3:PO_4 at day 14 compared to control (Figure S6F-G). This model exhibited no changes internally and externally for the 1670/1640 ratio nor with the 960 cm^{-1} peak width (Figure S6I-J).

Administration of NH_4Cl influences whole bone femur mechanics

Three-point bending of the femur (Figure 3A-B) was used to evaluate whether acid-loading influences whole bone mechanics. In the graded-dose group, toughness increased from day 1 (5.264 MPa) today 14 (7.060 MPa) (Figure 3E). Additionally, resilience increased from days 1 and 14 and between days 3 and 14 in the graded-dose group (Figure 3F). The other structural and material mechanical properties, such as maximum load and modulus, were not altered in this model (Figure 3C-D). The flat-dose group did not exhibit any changes in material, such modulus, nor structural, such as maximum load, mechanical properties at any time point evaluated compared to its control group (Figure S8).

Structural analysis revealed early changes in trabecular bone

µCT was employed to examine acid-dosing effects on the structure and geometry of the trabecular bone in the femoral epiphysis (Figure 4A) and distal shaft (Figure 4D) as well as the midshaft cortical bone (Figure 4G). Bone parameters were altered in response to gradation and duration of acid-loading in the trabecular bone. The graded-dose diet altered the bone structure. The femurs exhibited a trending decrease in epiphyseal trabecular bone volume (BV/TV) for day 1 compared to its control (Figure 4C). The Tb.N significantly decreased at day 3 in the graded-dose group (Figure 4C). Neither the diaphyseal trabecular bone nor the cortical indices showed no measurable changes in the graded-dose model of MA. The flat-dose group did not exhibit any significant changes in the cortical or epiphyseal trabecular structural metrics at any time point (Figure S9). However, the distal shaft increased in bone volume (BV/TV) and trabecular number (Tb.N) as well as decreased in trabecular separation (Tb.Sp) at the early timepoints compared to its respective control group (Figure S9D).

How to cite this article: Mikayla M, Anna P, Brian W, Katya M, Iris N, et al. Physiochemical Dissolution Governs Early Modifications in Acid-Exposed Murine Bone with Long-term Recovery. Ortho & Rheum Open Access J. 2023; 22(1): 556076. DOI: 10.19080/OROAJ.2023.22.556076

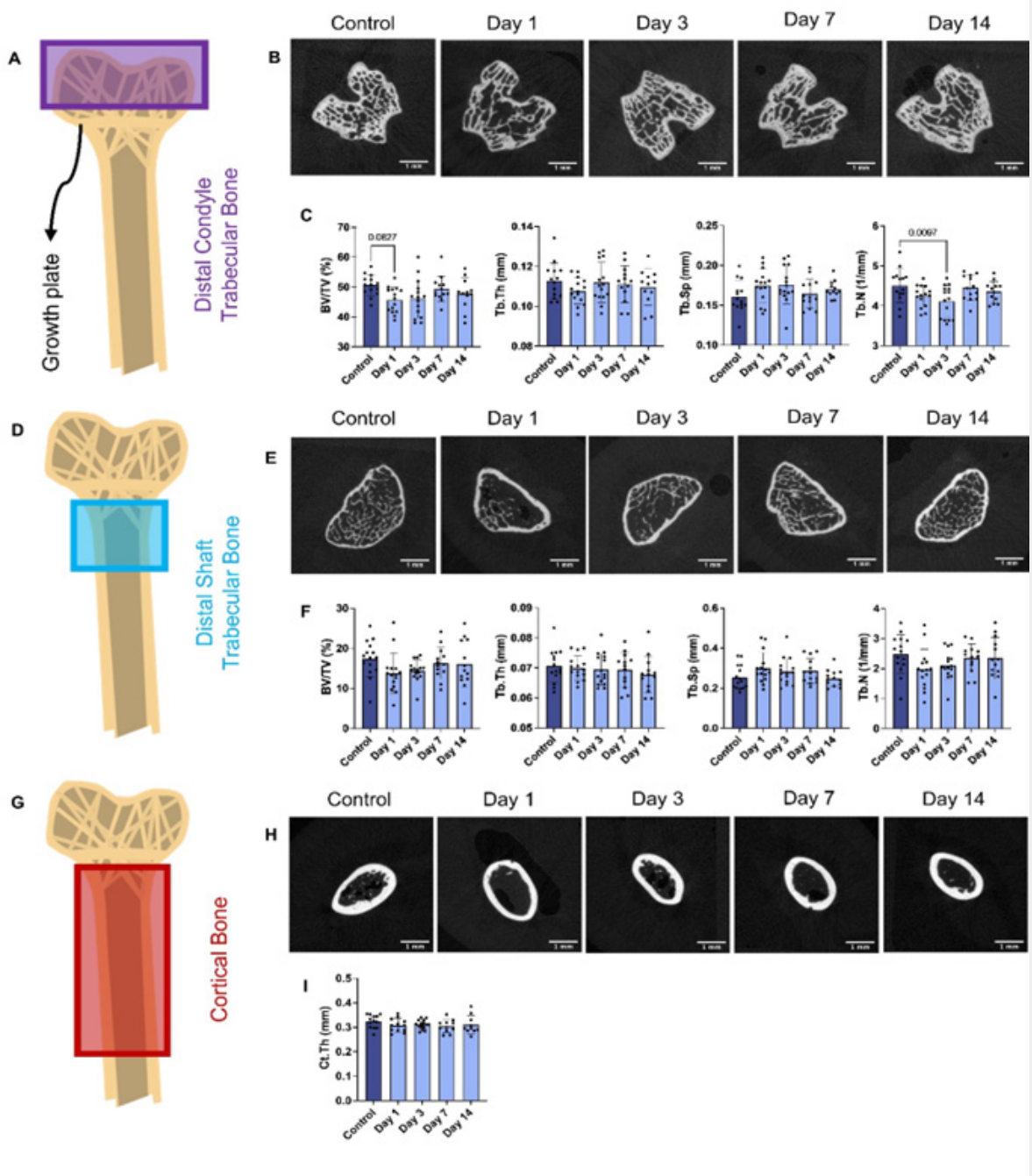

Figure 4: Slight reduction in trabecular bone in condyles of early acid-exposed bone. (A) A schematic showing the Region of Interest (ROI) of trabecular analysis inside the condyles. (B) Images of condyles. (C) Distal condyle trabecular bone parameters calculated during analysis. (D) A schematic showing the ROI of trabecular analysis within the distal shaft. (E) Images of distal shaft. (F) Distal shaft trabecular bone parameters calculated during analysis. (G) A schematic showing the ROI of cortical analysis in the shaft. (H) Images of shaft. (I) Shaft cortical bone parameters calculated during analysis. One-way ANOVAs and post-hoc Tukey's tests were used. P values less than or equal to 0.1 are reported.

Lack of cellular bone resorption in ammonium chloride MA models

Mineral apposition and erosion were determined by bone calcein/alizarin dynamic histomorphometry (Figure 5A). For all femurs, the single labeled surfaces, double labeled surfaces, mineral apposition rate, and bone formation rate did not significantly change compared to their respective controls (Figsure 5B-E & S10A-D). We also assessed how the dosing and duration of NH_4Cl administration influenced femur osteoclast

How to cite this article: Mikayla M, Anna P, Brian W, Katya M, Iris N, et al. Physiochemical Dissolution Governs Early Modifications in Acid-Exposed Murine Bone with Long-term Recovery. Ortho & Rheum Open Access J. 2023; 22(1): 556076. DOI: 10.19080/OROAJ.2023.22.556076

(OC) activity by traditional TRAP histological staining and quantification of TRAP+-area and cells (Figure 5F). However, the TRAP-surface, cell number, or eroded surface in the femur did not significantly change for the flat-dose nor the graded-dose groups (Figure 5G-J & S10E-H).

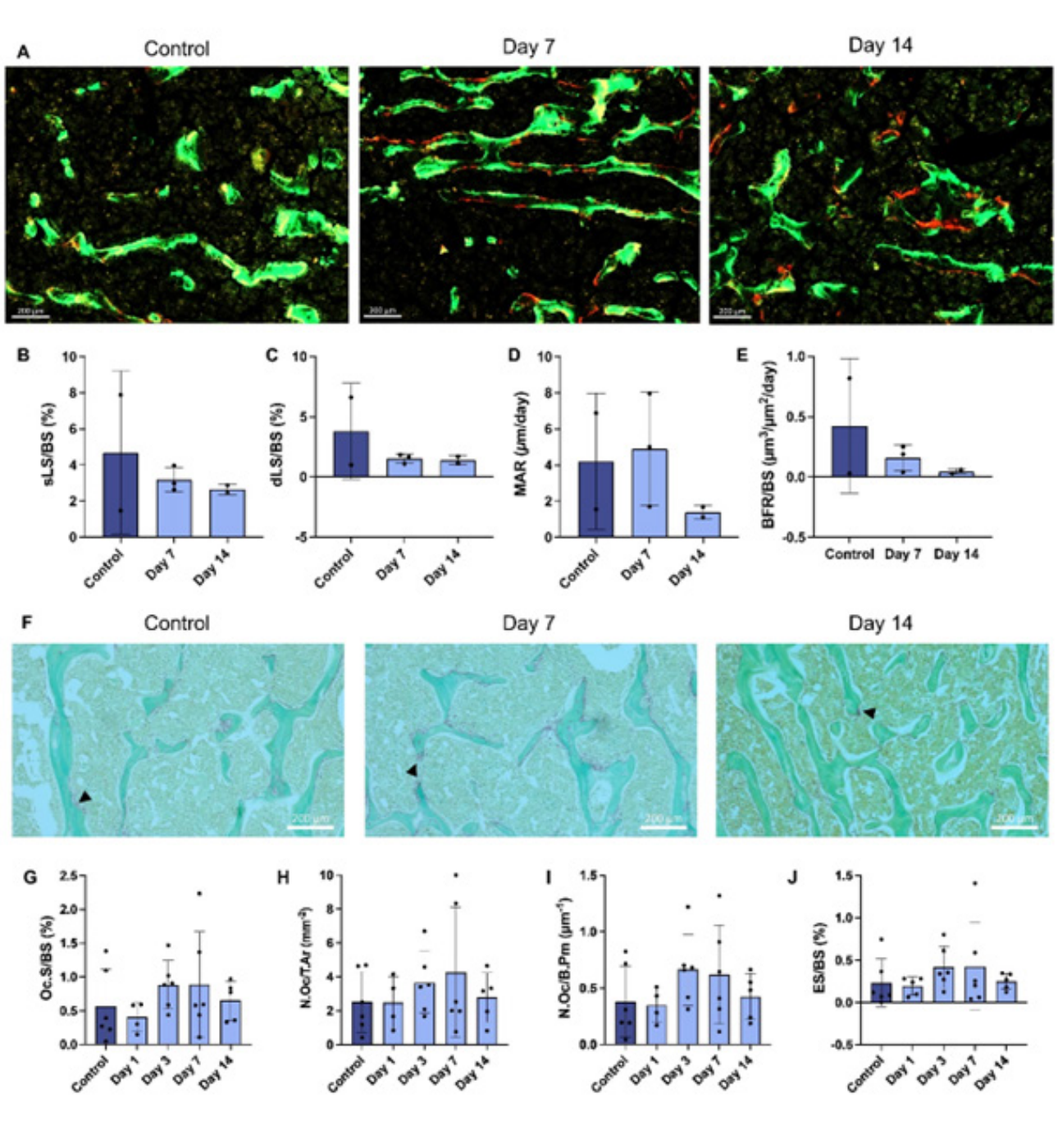

Figure 5: Slight reduction in trabecular bone in condyles of early acid-exposed bone. (A) A schematic showing the Region of Interest (ROI) of trabecular analysis inside the condyles. (B) Images of condyles. (C) Distal condyle trabecular bone parameters calculated during analysis. (D) A schematic showing the ROI of trabecular analysis within the distal shaft. (E) Images of distal shaft. (F) Distal shaft trabecular bone parameters calculated during analysis. (G) A schematic showing the ROI of cortical analysis in the shaft. (H) Images of shaft. (I) Shaft cortical bone parameters calculated during analysis. One-way ANOVAs and post-hoc Tukey's tests were used. P values less than or equal to 0.1 are reported.

How to cite this article: Mikayla M, Anna P, Brian W, Katya M, Iris N, et al. Physiochemical Dissolution Governs Early Modifications in Acid-Exposed Murine Bone with Long-term Recovery. Ortho & Rheum Open Access J. 2023; 22(1): 556076. DOI: 10.19080/OROAJ.2023.22.556076

Discussion

Clinically, metabolic acidosis is characterized by a decrease in serum pH and HCO_3-, which can cause bone dissolution and lead to reduced BMD and increased rates of fracture [1-4]. With increased incidence of acidosis, it is becoming essential to understand the process by which acidosis induces bone damage *in vivo*. Current murine models of MA center on the either flat-dose or graded-dose administration of NH_4Cl via the drinking water [13,20,22]. However, the dose and time dependence of these models on bone quality remain unclear. Acidosis-induced changes in bone appear to be caused by either physiochemical or cell-mediated processes, but the relative effects of these processes on bone quality and function as a function of time are unknown. Here we apply a multi-technique approach to understanding the temporal consequences of acidosis on bone quality and function in both the flat-dose and graded-dose MA models.

Dosing regimen of acid-loading is critical for long-term MA induction

The ability of the flat-dose and graded-dose murine models of MA to induce and maintain acidosis up to 14 weeks was determined using blood and urine measures. The graded-dose model maintained the decreased blood pH out to days 7 and 14. This onset of acidemia, define as reduce blood pH, was accompanied by a concurrent decrease in HCO_3- at days 1, 7, and 14, indicating that the model can induce chronic metabolic acidosis in CD-1 male adult mice up to 14 days. This more closely mimics clinical MA in humans [56,57] and supports the relevance of the graded-dose model [22]. For the flat-dose model, in which 0.28 M NH_4Cl was continuously administered [13,18,20], we found that blood pH only decreased at day 1 and HCO_3- levels were unaffected compared to controls. This indicates that the flat-dose model in CD-1 mice was unable to induce acidosis and that only acidemia, reduction in blood pH by not HCO_3-, was induced at day 1. Other studies have similarly shown an inability to maintain murine MA beyond a few days using a flat-dose model [18], but not to the same extent as we see here. This discrepancy may result from the different mouse strains used in this study (CD-1) and others (C57Bl/6J). Overall, these results indicate that the graded-dose model is appropriate as a long-term model of MA in CD-1 male adult mice, while the flat-dose model fails to induce acidosis.

Interestingly, with the inclusion of additional time points in the current study, we saw blood pH and HCO_3- return to baseline levels at day 3 in the graded-dose model, despite the decrease on days 1, 7, and 14. Although this result was unexpected, patients with chronic kidney disease and concomitant MA commonly experience eubicarbonatemic metabolic acidosis (EMA), where their blood pH and HCO_3- levels are normal but they exhibit ongoing H+ ion retention [50,58,59]. To determine whether the graded-dose mice exhibit EMA or if this return to baseline at day 3 is caused by other variables, we assessed consumption and urine-based factors. We found that consumption volume of the drinking water remained constant for the NH_4Cl doses during this time period (0.2 and 0.3 M). This, in addition to the elevated blood Cl^- levels, indicates that changes in NH_4Cl intake were not the reason for the lack of acidosis on day 3. Urine pH of the graded-dose mice remained acidic and unchanged throughout the 14 days compared to the control. This suggests that acid-wasting via urinary excretion was unaltered and thus fails to explain the day 3 blood gas results [60]. Having excluded NH_4Cl consumption and acid wasting as possible factors, the pH and HCO_3- increase at day 3 points to the development of EMA due to activation of compensatory buffering mechanisms. We predict that these mechanisms center on dissolution of bone tissue and release of buffering ions, temporarily restoring blood pH and HCO_3- to normal values [59-62]. The increasing doses of NH_4Cl in the graded-dose model past day 3 overcome this compensatory response, allowing for continued clinical MA at longer time points. Overall, we demonstrated that the graded-dose model is more effective in exhibiting clinically translatable MA symptoms than the flat-dose model in CD-1 male mice and that there are strong temporal responses to acidosis.

Chronic acidosis significantly affects bone matrix composition and structure

Having established that the models induce time-dependent acidemia or acidosis and that these conditions may be inhibited by compensatory mechanisms, we were interested in examining the effect of each model on bone dissolution and thus buffering ion release. Both the flat-dose and graded-dose models exhibited an increase in blood Ca^{2+} and Na^+ ions with an NH_4Cl challenge. The stronger correlation between blood pH and Ca^{2+} (C=-0.41) as compared to HCO_3- and Ca^{2+} (C=-0.28) suggests that the calcium release is primarily being controlled by changes in pH. Increased blood Ca^{2+} and Na^+ levels are used as indicators of bone dissolution [50,51], this points to reduced pH promoting bone dissolution. Examination of the effect of possible acid-induced dissolution on the bone was performed using a multi-technique approach to characterize structural and compositional modifications to the flat-dose and graded-dose murine bones.

Modifications in bone composition are commonly observed in acidic microenvironments, spanning acidic cancerous environments to biomineral exposure to acidic media [63,64]. Femurs from the graded-dose model exhibited significant compositional changes at early time points. The mineral: matrix ratio decreased in the interior of the femurs at nearly all time points, suggesting rapid onset of mineral dissolution upon induction of MA. There was a negative correlation (C=-0.15) between the interior and exterior mineral matrix that could suggest a preferential dissolution of the interior over the exterior bone. This reduction in mineral content is also accompanied by an early decrease in the CO_3:PO_4 ratio of the remaining mineral

How to cite this article: Mikayla M, Anna P, Brian W, Katya M, Iris N, et al. Physiochemical Dissolution Governs Early Modifications in Acid-Exposed Murine Bone with Long-term Recovery. Ortho & Rheum Open Access J. 2023; 22(1): 556076. DOI: 10.19080/OROAJ.2023.22.556076

at days 1 and 3. Acting as a strong buffer, carbonate removal from the bone mineral has been previously reported *in vivo*, ex vivo, and *in vitro* in response to acidic environments [22,36,63,65]. Interestingly, its removal is associated with a narrowing in the width of the 960cm^{-1} peak, indicating an increase in mineral crystallinity at days 1 and 3. A combination of decreased CO_3^{2-} and increased crystallinity indicates physiochemical mineral dissolution/recrystallization [36,66,67]. In the case of increased remodeling, simultaneous decrease of both CO_3^{2-} and crystallinity would be expected [68,69]. This suggests that the mineral loss seen at days 1 and 3 is likely caused by physiochemical dissolution and reprecipitation mechanisms. This improvement in bone mineral crystallinity at early timepoints will reduce its solubility, thus inhibiting further dissolution of bone mineral as well as possibly acting as a negative feedback loop to regulate bone mineral loss [70]. This early carbonate loss at days 1 and 3 may explain the elevated pH and HCO_3- seen at day 3, while the subsequent return to acidic pH afterwards may be a consequence of reduced mineral solubility from day 3. In addition, the width of the 1450 cm^{-1} peaks significantly widened at days 1 and 3, which is associated with reduced atomic ordering of the CH_2 bonds in the organic matrix. This suggests that the graded dosing causes degradation or denaturation of the organic matrix [71]. This process is reversed at later time points possibly due to increased fibrillogenesis in the presence of elevated Cl^- ions [72,73]. Together, these results indicate that there are significant interactions between acidic body fluids and bone composition that vary with time and possibly act as a physiochemical feedback loop to inhibit excessive bone loss, providing a key factor in understanding the body's ability to regulate acidosis.

Structurally, the trabecular bone exhibited a trending decrease in BV/TV at day 1 and a significant decrease in Tb.N at day 3 compared to the control, suggesting bone loss at the early time points. Although this rapid bone loss parallels the rapid decrease in mineral and increase in collagen denaturation seen in the Raman data, this can seem like an overly significant result for such a short time span. However, rapid bone loss is not uncommon, as seen in animal studies looking at the effects of radiation [74], COVID-19 [75], and spinal cord injuries [76] on bone. In addition, due to the high permeability of bone and high dissolution rate of bone minerals it is possible that these physiochemical processes act quickly [77,78]. Contrarily, the diaphyseal trabecular bone did not show any changes. The epiphyseal results were like studies looking at acidosis in rats via NH_4Cl administration, where bone resorption was higher in the epiphysis than the diaphysis of the tibia [79]. However, our results were also different compared to studies done in ovariectomized rats, which found decreased trabecular bone within the metaphysis and a lack of change within the epiphysis [80,81]. The mechanistically different remodeling behaviors present within the epiphysis and diaphysis between our present study and other studies might be due to the trabecular structural differences between rats and mice as well sex-based differences (female vs. male) [82].

In the flat-dose bones, we found that the CO_3:PO_4 ratio decreased in the bone interior at day 1 suggesting a decrease in carbonate content in response to the acidemia which was recovered once the pH returned to baseline. Structurally, the diaphyseal trabecular parameters BV/TV and Tb.N increased at day 7, indicating that bone growth occurred even with acid exposure. Taken together, this data suggests that the short-term acidemia induced by the flat-dose model was not sufficient to cause any major bone loss or compositional changes compared to controls. The lack of tissue loss during this time suggests that remodeling processes may not have been impaired due to acidosis. In comparison, the lack of bone growth in the graded-dose group points to acid-exposure potentially deterring bone formation. These results further iterate that the graded-dose regimen mimics altered bone phenotypes seen in clinical metabolic acidosis while the flat-dose model is not sufficient to mimic long-term MA. In addition, there is a temporal response to the acid induction with physiochemical processes that have rapid effects on bone composition and structure.

Early changes in bone structure and composition during MA are not cell-mediated

Although structural and compositional data point to primarily physiochemical processes, it was important to address both physiochemical dissolution and the possible cell-mediated resorption [35]. Cellularly, *in vitro* studies have shown that acidic media leads to increased osteoclastogenesis as well as osteoclast activity [30-32,83,84]. This has also been seen in certain *in vivo* experiments [14]. However, our previous work using the graded-dose model showed a decrease in osteoclast numbers after 14 days of acidosis compared to controls, potentially due to an increase in blood HCO_3- levels [22]. Thus, cellular characterization was performed to understand the role that cellular activity may play in the measured compositional and structural changes as a function of time.

As osteoclasts are the primary cells responsible for resorption, we focused on examining the temporal effects of MA on the number and activity of TRAP+-cells. Histologically, we did not see any significant change in osteoclast numbers at any time points via TRAP staining in either the flat-dose or the graded-dose model in agreement with Meghji et al. [32] who observed no change in osteoclast number but a marked increase in their activity. However, neither model in this study exhibited an increase in osteoclast activity, as illustrated by the lack of change in eroded surface. This lack of osteoclast response may be due to an insufficient change in pH to promote differentiation or activation. Previous studies showing an increase in osteoclast number and activity, had significantly larger reductions in pH than those measured in this study, some reaching a pH of 6.8 [29,32]. In addition, 14 days may not be sufficient to measure significant osteoclast activation and longer timepoints should be investigated.

How to cite this article: Mikayla M, Anna P, Brian W, Katya M, Iris N, et al. Physiochemical Dissolution Governs Early Modifications in Acid-Exposed Murine Bone with Long-term Recovery. Ortho & Rheum Open Access J. 2023; 22(1): 556076. DOI: 10.19080/OROAJ.2023.22.556076

To further clarify the role that cellular remodeling might play on the structural and compositional response of bone to MA, we performed dynamic histomorphometry on the samples. Despite the small sample numbers, looking at single labeled surface, double labeled surface, mineral apposition rate (MAR), and bone formation rate (BFR/BS), the flat-dose and graded-dose groups showed no changes at any time points. This agrees with the lack of change in diaphyseal trabecular bone, especially in the graded-dose model. However, the lack of remodeling presented by the dynamic histomorphometry data suggests that there was no significant cellular contribution to the MA response of bones in either the flat-dose or graded-dose models. This was expected since we saw no changes in TRAP+-cell number or activity. Due to the lack of bone formation after apparent bone loss indicated by Tb.N and BV/TV as well as bone dissolution of Ca^{2+}, Na^{+}, and HCO_3-, this further suggests that changes in the bone are likely dominated by physiochemical processes at early timepoints of acidosis.

Bone toughness is slightly altered with acidosis

Three-point bend testing of the graded-dose bones showed no differences in any mechanical parameters compared to control. However, resilience and toughness significantly increase between days 1 and 3 and day 14. This difference between early and late acidosis time points suggests that acidosis may cause an initial decrease in the tissue toughness/resilience followed by an increase at 14 days. Due to the positioning of the bone in 3-point bend, such that the crack propagates through the structurally unchanged cortical mid-shaft, we do not expect that these changes in mechanics are caused by macro-scale structural modifications but by compositional and small-scale structural changes instead. The change in toughness is most significantly correlated to the measure of collagen disorder on the bone exterior (1450 width C=0.42). Such changes in collagen order or structure have been associated with decreased tissue toughness [52,55]. The mechanical changes between days 1 and 14 are mirrored by increased carbonate content and decreased crystallinity at the bone surface as shown by the increase in CO_3:PO_4 and 960 peak widths between the two timepoints. These compositional changes point to an initial stiffening of the apatite crystals at early timepoints followed by an increase in crystal compliance at day 14 [37].

Stiffening of the mineral reinforcing phase at early timepoints could result in decreased tissue toughness seen here due to reduced crack deflection and increased reinforcement cracking [85,86]. This suggests that the tissue toughness is primarily controlled by the quality of the collagen and mineral on the bone surface. Indeed, it is expected during 3pt bending that a crack will form on the tensile surface of the cortical bone. If the collagen at that bone surface exhibits a more disordered and less plastic organic matrix along with a stiffened mineral reinforcement, crack propagation would be facilitated, and toughness reduced. The decrease in tissue toughness in response to changes in bone composition after an acidic challenge may explain the clinically observed increased fracture risk in patients with acidosis [87].

Beyond the change in toughness, we saw no changes in tissue strength or stiffness, which disagrees with our previous work that found a decrease in bone maximum load [22]. The decrease in maximum load in our previous study was caused by an associated decrease in the cortical bone geometry not paralleled here. As the current study was modified to be a time course study, we believe that the repeat *in vivo* blood draws in our initial study caused the acidosis induction to have a more significant effect on the murine metabolism, and the increase of blood loss led to the differing bone structure and subsequent change in mechanics reported in our prior study. By eliminating the repeated blood draws and significant blood loss in our current study, we expect that this study more clearly investigates the effect of acidosis on the skeletal system as observed in non-surgical procedures and minimizes the compounded influence of altered hematopoiesis [47]. 3-point bend testing indicated that flat-dose bones exhibited no change in mechanical properties at any time points. Overall, these results show that compositional changes induced by acidosis can induce significant time-dependent mechanical changes in the bone.

Limitations

Although this study was able to determine the temporal effects of a flat and graded dosing NH_4Cl regimens on the structural, compositional, and mechanical properties of murine bone, like all animal studies it has some limitations. First, due to the age and skeletal maturity of the mice and experimental time, we did not expect that there would be any changes in the bone properties in the control group over the course of the experiment. Therefore, a single control group was selected instead of providing a control group for every timepoint. Although the latter could have provided better comparisons between controls and acidosis, the number of mice needed to do so would have been prohibitive, especially considering the small, expected changes.

Secondly, even though the blood pH and HCO_3- remained low after 14 days of MA induction, the bones only experienced changes in the first three days. We propose that this could be caused by a compositional feedback loop but there could also be other participating factors. Although osteoblast activity has generally been shown to decrease with acidosis [29,33], no osteoblastic measurements were made here. However, dynamic histomorphometry showed no significant changes with acidosis suggesting that this may not be cellularly controlled. Despite this, further biological examinations, such as RNA-Seq, could provide an interesting broader understanding of the cellular response.

In addition, in the graded dose model, the mice consumed lower volumes of the solutions as the concentration of the NH_4Cl

How to cite this article: Mikayla M, Anna P, Brian W, Katya M, Iris N, et al. Physiochemical Dissolution Governs Early Modifications in Acid-Exposed Murine Bone with Long-term Recovery. Ortho & Rheum Open Access J. 2023; 22(1): 556076. DOI: 10.19080/OROAJ.2023.22.556076

increased. This limits the usefulness of the model at timepoints beyond 14 days where consumption may be too low to reasonably maintain mouse health. This could be overcome by either adding NH_4Cl to food and drinking water or by switching to gavage feeding of NH_4Cl. Lastly, the flat-dose and graded-dose models were performed at different times in different institutions. Controls are appropriate for each model type therefore we do not expect any issues within a single model. In addition, 4-6-month-old CD-1 male mice from the same supplier were used for both models. However, differences in animal husbandry, sample preparation, and experimental design could have led to some of the differences seen between the flat dose and the graded dose models.

Conclusion

This study shows that unlike the flat-dose model, graded administration of NH_4Cl temporally affected the bone matrix composition and structure. At early time points, the bone exhibited a decrease in mineral content as well as compositional changes to the mineral, including decreased carbonate content and increased crystallinity. Concurrently, the collagen matrix exhibited a decrease in atomic order, suggesting a certain extent of collagen degradation. These time-dependent compositional changes were associated with alterations in tissue resilience and toughness that could lead to the increased fracture risk seen clinically. Thus, our study indicates that one must consider the temporal and dosage effects of exogenous acid on the material properties of bone. We believe our graded-dose model will help lead to a better understanding of the bone dissolution mechanisms of MA, and in the long-term, to the discovery of better treatments.

References

1. D A Bushinsky (2001) Acid-base imbalance and the skeleton. Eur J Nutr 40(5): 238–244.
2. J Lemann, J R Litzow, E J Lennon (1966) The effects of chronic acid loads in normal man: further evidence for the participation of bone mineral in the defense against chronic metabolic acidosis. J Clin Invest 45(10): 1608-1614.
3. J Lemann, D A Bushinsky, L L (2003) Hamm, Bone buffering of acid and base in humans. Am J Physiol Renal Physiol 285(5): F811–F832.
4. T R Arnett (2010) Acidosis, hypoxia and bone. Arch Biochem Biophys 503(1): 103–109.
5. AM Wu, C Bisignano, SL James, GG Abady, A Abedi E, et al. (2021) Global, regional, and national burden of bone fractures in 204 countries and territories, 1990–2019: a systematic analysis from the Global Burden of Disease Study 2019. Lancet Healthy Longev 2(2021): e580–e592.
6. R K Hernandez, A Adhia, S W Wade, E O'Connor, J Arellano, et al. (2015) Prevalence of bone metastases and bone-targeting agent use among solid tumor patients in the United States. Clin Epidemiol 7: 335-345.
7. M Bonafede, D Espindle, AG Bower (2013) The direct and indirect costs of long bone fractures in a working age US population, J Med Econ 16(1): 169–178.
8. M Hagiwara, A Oglesby, K Chung, S Zilber, TE Delea (2011) The impact of bone metastases and skeletal-related events on healthcare costs in prostate cancer patients receiving hormonal therapy. Community Oncology 8(11): 508–515.
9. T R Arnett, D W Dempster (1986) Effect of pH on bone resorption by rat osteoclasts *in vitro*. Endocrinology 119(1): 119–124.
10. S Meghji, M S Morrison, B Henderson, T R Arnett (2001) pH dependence of bone resorption: Mouse calvarial osteoclasts are activated by acidosis. Am J Physiol Endocrinol Metab 280(1): E112–E119.
11. D A Bushinsky (1995) Stimulated osteoclastic and suppressed osteoblastic activity in metabolic but not respiratory acidosis. Am J Physiol 268(1995): C80–C88.
12. D A Bushinsky, B C Lam, R Nespeca, N E Sessler, M D Grynpas (1993) Decreased bone carbonate content in response to metabolic, but not respiratory, acidosis. Am J Physiol 265(1993): F530-536.
13. N S Krieger, K K Frick, D A (2004) Bushinsky, Mechanism of acid-induced bone resorption. Current Opinion in Nephrology and Hypertension 13(4): 423–436.
14. M M Moynahan, S L Wong, A C Deymier (2021) Beyond dissolution: Xerostomia rinses affect composition and structure of biomimetic dental mineral *in vitro*. PLoS One 16(4): e0250822.
15. B Wingender, M Azuma, C Krywka, P Zaslansky, J Boyle, et al. (2021) Carbonate substitution significantly affects the structure and mechanics of carbonated apatites. Acta Biomater 122: 377–386.
16. D A Bushinsky, R Levi-Setti, F L Coe, (1986) Ion microprobe determination of bone surface elements: effects of reduced medium pH. Am J Physiol 250(2): F1090-1097.
17. DA Bushinsky, NS Krieger, DI Geisser, EB Grossman, FL Coe, et al. (1983) Effects of pH on bone calcium and proton fluxes *in vitro*. Am J Physiol 245(2): F204–F209.
18. Y Li, A Asadi, M R Monroe, E P Douglas (2009) pH effects on collagen fibrillogenesis *in vitro*: Electrostatic interactions and phosphate binding. Materials Science and Engineering C 29(5): 1643–1649.
19. A E Russell (1974) Effect of pH on thermal stability of collagen in the dispersed and aggregated states, Biochem J 139(1): 277–280.
20. D A Bushinsky (1994)Acidosis and bone, Miner Electrolyte Metab 20(1-2): 40–52.
21. A M Sharma, A Distler (1994) Acid-base abnormalities in hypertension. Am J Med Sci S112-115.
22. D Aryal, T Roy, JC Chamcheu, KE Jackson (2020) Chronic Metabolic Acidosis Elicits Hypertension via Upregulation of Intrarenal Angiotensin II and Induction of Oxidative Stress. Antioxidants (Basel) 10(1): 2.
23. Z Rumbus, E Toth, L Poto, A Vincze, G Veres, et al. (2018) Garami, Bidirectional Relationship Between Reduced Blood pH and Acute Pancreatitis: A Translational Study of Their Noxious Combination, Frontiers in Physiology 9: 1360.
24. H J Kim (2021) Metabolic Acidosis in Chronic Kidney Disease: Pathogenesis, Clinical Consequences, and Treatment. Electrolyte Blood Press 19(2): 29–37.
25. W T Golde, P Gollobin, LL Rodriguez (2005) A rapid, simple, and humane method for submandibular bleeding of mice using a lancet. Lab Anim (NY) 34(9): 39–43.
26. N A Dyment, X Jiang, L Chen, S H Hong, D J Adams, et al. (2016) High-Throughput, Multi-Image Cryohistology of Mineralized Tissues. J Vis

How to cite this article: Mikayla M, Anna P, Brian W, Katya M, Iris N, et al. Physiochemical Dissolution Governs Early Modifications in Acid-Exposed Murine Bone with Long-term Recovery. Ortho & Rheum Open Access J. 2023; 22(1): 556076. DOI: 10.19080/OROAJ.2023.22.556076

Exp 115: 54468.

27. M Doube, M M Kłosowski, I Arganda-Carreras, F P Cordelieres, R P Dougherty, et al. (2010) Bone J: Free and extensible bone image analysis in ImageJ. Bone 47(6): 1076–1079.

28. AD Renaghan, MH Rosner (2018) Hypercalcemia: etiology and management, Nephrology Dialysis Transplantation. NDT 33(4): 549–551.

29. W H Bergstrom, F D Ruva (1960) Changes in bone sodium during acute acidosis in the rat. Am J Physiol 198: 1126–1128.

30. M Unal, H Jung, O Akkus (2015) Novel Raman Spectroscopic Biomarkers Indicate that Post-Yield Damage Denatures Bone's Collagen. J Bone Miner Res 31(5): 1015-1025.

31. M D Morris, G S Mandair (2011) Raman Assessment of Bone Quality. Clin Orthop Relat Res 469(8): 2160–2169.

32. B Wopenka, A Kent, J D Pasteris, Y Yoon, S Thomopoulos (2008) The Tendon-to-Bone Transition of the Rotator Cuff: A Preliminary Raman Spectroscopic Study Documenting the Gradual Mineralization Across the Insertion in Rat Tissue Samples. Appl Spectrosc 62(12): 1285–1294.

33. M Unal, S Uppuganti, S Timur, A Mahadevan-Jansen, O Akkus, et al. (2019) Assessing matrix quality by Raman spectroscopy helps predict fracture toughness of human cortical bone. Sci Rep 9: 7195.

34. J J DiNicolantonio, J O'Keefe (2021) Low-grade metabolic acidosis as a driver of chronic disease: a 21st century public health crisis. Open Heart 8(2): e001730.

35. R A Carnauba, A B Baptistella, V Paschoal, G H Hubscher (2017) Diet-Induced Low-Grade Metabolic Acidosis and Clinical Outcomes: A Review. Nutrients 9(6): 538.

36. N E Madias (2021) Eubicarbonatemic Hydrogen Ion Retention and CKD Progression. Kidney Medicine 3(4): 596–606.

37. N E Madias (2021) Metabolic Acidosis and CKD Progression, Clin J Am Soc Nephrol 16(2): 310.

38. L F Boswald, D Matzek, E Kienzle, B Popper (2021) Influence of Strain and Diet on Urinary pH in Laboratory Mice, Animals (Basel) 11(3): 702.

39. K L Raphael (2018) Metabolic Acidosis and Subclinical Metabolic Acidosis in CKD. J Am Soc Nephrol 29(2): 376–382.

40. D E Wesson, J M Buysse, D A Bushinsky (2020) Mechanisms of Metabolic Acidosis-Induced Kidney Injury in Chronic Kidney Disease, J Am Soc Nephrol 31(3): 469–482.

41. D A Bushinsky, S B Smith, K L Gavrilov, L F Gavrilov, J Li, et al. (2002) Acute acidosis-induced alteration in bone bicarbonate and phosphate, American Journal of Physiology-Renal Physiology 283(5): F1091–F1097.

42. C Zhang, P T W Jr, S Dasari, S L Kominsky, M Doucet, S Jayaraman, et al. (2018) Label-free Raman spectroscopy provides early determination and precise localization of breast cancer-colonized bone alterations. Chem Sci 9(3): 743–753.

43. D A Bushinsky, J M Chabala, K L Gavrilov, R Levi-Setti (1999) Effects of *in vivo* metabolic acidosis on midcortical bone ion composition, American Journal of Physiology-Renal Physiology. 277(5): F813–F819.

44. A A Baig, J L Fox, J Hsu, Z Wang, M Otsuka, et al. (1996) Effect of Carbonate Content and Crystallinity on the Metastable Equilibrium Solubility Behavior of Carbonated Apatites. Journal of Colloid and Interface Science 179: 608–617.

45. S V Dorozhkin (2012) Dissolution mechanism of calcium apatites in acids: A review of literature. World J. Methodol 2(1): 1–17.

46. A L Boskey, L Imbert (2017) Bone quality changes associated with aging and disease: a review. Ann N Y Acad Sci 1410(1): 93–106.

47. A L Boskey, R Coleman (2010) Aging and bone. J Dent Res 89(12): 1333–1348.

48. A C Deymier, A K Nair, B Depalle, Z Qin, K Arcot, et al. (2017) protein-free formation of bone-like apatite: New insights into the key role of carbonation, Biomaterials. 127: 75–88.

49. C D Flanagan, M Unal, O Akkus, C M Rimnac (2017) Raman spectral markers of collagen denaturation and hydration in human cortical bone tissue are affected by radiation sterilization and high cycle fatigue damage, J Mech Behav Biomed Mater 75: 314–321.

50. J R Harris, A Soliakov, R J Lewis (2013) *in vitro* fibrillogenesis of collagen type I in varying ionic and pH conditions, Micron 49: 60–68.

51. A R McCluskey, K S W Hung, B Marzec, J O Sindt, N A J M Sommerdijk, et al. (2020) Disordered Filaments Mediate the Fibrillogenesis of Type I Collagen in Solution, Biomacromolecules. 21(9): 3631–3643.

52. D Jia, D Gaddy, L J Suva, P M Corry (2011) Rapid Loss of Bone Mass and Strength in Mice after Abdominal Irradiation. Radiat Res 176(5): 624–635.

53. A K Haudenschild, B A Christiansen, S Orr, E E Ball, C M Weiss, et al. (2023) Haudenschild, Acute bone loss following SARS-CoV-2 infection in mice. J Orthop Res.

54. Y Peng, W Zhao, Y Hu, F Li, X E Guo, et al. (2020) Rapid bone loss occurs as early as 2 days after complete spinal cord transection in young adult rats. Spinal Cord 58(3): 309–317.

55. C R Hankermeyer, K L Ohashi, D C Delaney, J Ross, B R Constantz, et al. (2002) Dissolution rates of carbonated hydroxyapatite in hydrochloric acid, Biomaterials 23(3): 743–750.

56. T Beno, Y J Yoon, S C Cowin, S P Fritton (2006) Estimation of bone permeability using accurate microstructural measurements, J Biomech 39(13): 2378–2387.

57. J A Kraut, D R Mishler, F R Singer, W G Goodman (1986) The effects of metabolic acidosis on bone formation and bone resorption in the rat. Kidney International 30(5): 694–700.

58. P A J Baldock, A G Need, R J Moore, TC Durbridge, H A Morris, et al. (1999) Discordance Between Bone Turnover and Bone Loss: Effects of Aging and Ovariectomy in the Rat, Journal of Bone and Mineral Research 14(8): 1442–1448.

59. RB Martin, SL Zissimos (1991) Relationships between marrow fat and bone turnover in ovariectomized and intact rats, Bone 12(2): 123–131.

60. C M Bagi, E Berryman, M R Moalli (2011) Comparative Bone Anatomy of Commonly used Laboratory Animals: Implications for Drug Discovery. Comp Med 61(1): 76–85.

61. F L Yuan, M H Xu, X Li, H Xinlong, W Fang, et al. (2016) The Roles of Acidosis in Osteoclast Biology. Front Physiol 7: 222.

62. A Carano, P H Schlesinger, N A Athanasou, S L Teitelbaum, H C Blair, et al. (1993) Acid and base effects on avian osteoclast activity, Am J Physiol 264(3): C694-701.

63. R O Ritchie (2011) The conflicts between strength and toughness, Nature Mater 10(11): 817–822.

64. R O Ritchie, M J Buehler, P Hansma (2009) Plasticity and toughness in bone. Physics Today 62: 41–47.

65. D E Sellmeyer, K L Stone, A Sebastian, S R Cummings (2001) A high ratio of dietary animal to vegetable protein increases the rate of bone loss and the risk of fracture in postmenopausal women. Study of Osteoporotic Fractures Research Group, Am J Clin Nutr 73(1): 118–122.

How to cite this article: Mikayla M, Anna P, Brian W, Katya M, Iris N, et al. Physiochemical Dissolution Governs Early Modifications in Acid-Exposed Murine Bone with Long-term Recovery. Ortho & Rheum Open Access J. 2023; 22(1): 556076. DOI: 10.19080/OROAJ.2023.22.556076

DOI: 10.19080/OROAJ.2023.22.556076

How to cite this article: Mikayla M, Anna P, Brian W, Katya M, Iris N, et al. Physiochemical Dissolution Governs Early Modifications in Acid-Exposed Murine Bone with Long-term Recovery. Ortho & Rheum Open Access J. 2023; 22(1): 556076. DOI: 10.19080/OROAJ.2023.22.556076